Regional Warming by Black Carbon and Tropospheric Ozone: A Review of Progresses and Research Challenges in China

LIAO Hong[1,2*] (廖 宏) and SHANG Jingjing[1,3] (尚晶晶)

1 *State Key Laboratory of Atmospheric Boundary Layer Physics and Atmospheric Chemistry, Institute of Atmospheric Physics, Chinese Academy of Sciences, Beijing* 100029

2 *Climate Change Research Center, Chinese Academy of Sciences, Beijing* 100029

3 *Graduate University of Chinese Academy of Sciences, Beijing* 100049

(Received November 24, 2014; in final form April 10, 2015)

ABSTRACT

Black carbon (BC) aerosol and tropospheric ozone (O_3) are major air pollutants with short lifetimes of days to weeks in the atmosphere. These short-lived species have also made significant contributions to global warming since the preindustrial times (IPCC, 2013). Reductions in short-lived BC and tropospheric O_3 have been proposed as a complementary strategy to reductions in greenhouse gases. With the rapid economic development, concentrations of BC and tropospheric O_3 are relatively high in China, and therefore quantifying their roles in regional climate change is especially important. This review summarizes the existing knowledge with regard to impacts of BC and tropospheric O_3 on climate change in China and defines critical gaps needed to assess the climate benefits of emission control measures. Measured concentrations of BC and tropospheric O_3, optical properties of BC, as well as the model estimates of radiative forcing by BC and tropospheric O_3 are summarized. We also review regional and global modeling studies that have investigated climate change driven by BC and tropospheric O_3 in China; predicted sign and magnitude of the responses in temperature and precipitation to BC/O_3 forcing are presented. Based on the review of previous studies, research challenges pertaining to reductions in short-lived species to mitigate global warming are highlighted.

Key words: black carbon, tropospheric ozone, radiative forcing, regional warming

Citation: Liao Hong and Shang Jingjing, 2015: Regional warming by black carbon and tropospheric ozone: A review of progresses and research challenges in China. *J. Meteor. Res.*, **29**(4), 525–545, doi: 10.1007/s13351-015-4120-0.

1. Introduction

The globally averaged combined land and ocean surface temperature exhibited a warming of 0.85 [0.65–1.06]℃ over 1880–2012, as reported by the Intergovernmental Panel on Climate Change (IPCC) Working Group I Fifth Assessment Report (AR5) (IPCC, 2013). Human activities contributed to changes in temperature through changing concentrations of both well-mixed greenhouse gases (WMGHGs, including carbon dioxide (CO_2), methane (CH_4), nitrous oxide (N_2O), and halocarbons) and short-lived species (nitrogen oxides (NO_x), carbon monoxide (CO), nonmethane volatile organic compounds (NMVOCs), tropospheric O_3, aerosols, and aerosol precursors). The radiative forcing (RF) values over 1750–2011 estimated by the IPCC AR5 are 3.00 W m^{-2} by emissions of WMGHGs and –0.64 W m^{-2} by emissions of short-lived species (Fig. 1), indicating that short-lived species also play important roles in climate change. Among the short-lived species, tropospheric O_3 is estimated to have a global mean RF of 0.40 W m^{-2}

Supported by the National (Key) Basic Research and Development (973) Program of China (2014CB441202) and Strategic Priority Research Program of the Chinese Academy of Sciences Strategic Priority Research Program (XDA05100503).

*Corresponding author: hongliao@mail.iap.ac.cn.

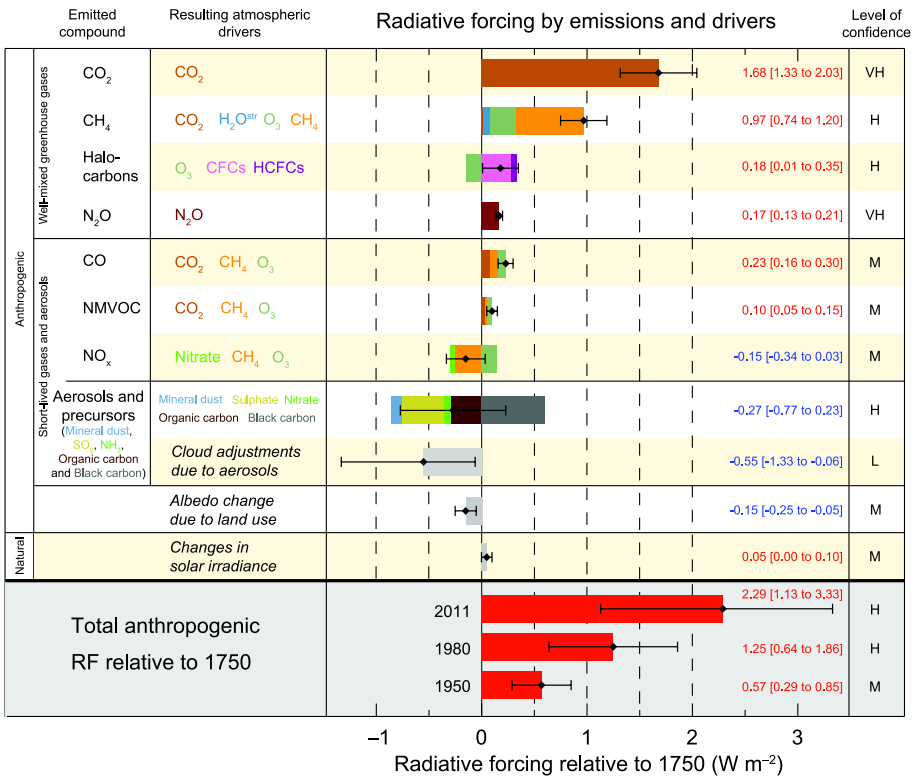

Fig. 1. Radiative forcing estimates in 2011 relative to 1750 and aggregated uncertainties for the main drivers of climate change. Positive (negative) radiative forcing indicates a warming (cooling) effect on climate. (Source: Figure SPM.5 of IPCC WGI AR5 Summary for Policymakers (IPCC, 2013))

(Table 8.6 in IPCC (2013)).

Short-lived species influence climate change in several ways depending on their chemical and physical properties. Firstly, the short-lived gases can influence concentrations of WMGHGs and aerosols by chemical reactions. For example, CO, NMVOCs, and NO_x are precursors of tropospheric O_3. Emissions of CO and NMVOCs lead to CO_2 formation in the atmosphere. Emissions of NO_x in the atmosphere influence concentrations of CH_4 by altering OH concentrations, and also contribute to nitrate aerosol formation. Secondly, some of the short-lived species, such as tropospheric O_3 and aerosols, exert radiative forcing to the energy balance of the earth's climate system. Tropopspheric O_3 is a greenhouse gas that leads to global warming (Fig. 1). Aerosols influence climate by interactions with radiation through scattering or absorbing of solar or longwave radiation, and by interactions with clouds through altering cloud properties. Major anthropogenic aerosol species in the atmosphere include sulfate, nitrate, ammonium, organic carbon (OC), and black carbon (BC), all of which have a cooling effect on climate except that BC has a warming effect. Thirdly, short-lived species participate in complex biogeochemical processes that can influence concentrations of WMGHGs. For example, the deposition of nitrogen and O_3 can influence carbon cycle by changing land cover (Lamarque et al., 2005; Janssens et al., 2010).

Due to the unidentified sinks for atmospheric CO_2, Jacobson (2005) assumed that CO_2 has a lifetime of 30–95 yr. Prather et al. (2012) derived that the present-day atmospheric lifetime is 9.1±0.9 yr for CH4 and 131±10 yr for N_2O. Tropospheric O_3 was reported to have a lifetime of about 3 weeks based on modeling studies (Liao and Seinfeld, 2005; Stevenson et al., 2006). Aerosols have even shorter lifetimes of several days (Kaufman et al., 2000). Jacobson (2004) compared the time-dependent changes in globally averaged near-surface temperature due to eliminating anthro-

pogenic emissions of each of CO_2, CH_4, as well as BC and OC from fossil fuel and biofuel sources. Considering that BC and OC were co-emitted species from anthropogenic and biomass burning sources, Jacobson (2004) suggested that the control of BC+OC may be the most effective method of slowing global warming for a specific period (about 10 yr), although OC itself has a cooling effect. The assessment report of United Nations Environment Programme (UNEP, 2011) proposed two approaches to mitigate global warming: one is to control the peak temperature by reducing the concentrations of short-lived species, such as BC, CH_4, and tropospheric O_3; the other is to control the long-term climate warming by reducing CO_2 concentrations. UNEP (2011) demonstrated by simulations of climate models that reductions in BC and tropospheric O_3 can be an effective method to slow the rate of climate change within the first half of this century. Climate benefits from reduced O_3 are achieved by reducing emissions of some of its precursors, especially methane that is also a powerful greenhouse gas.

With the rapid economic development, concentrations of short-lived species are relatively high in China; hence quantifying the role of short-lived species in regional and global climate change is especially important. Despite the complex interactions among WMGHGs and short-lived gases, this review is focused on BC and tropospheric O_3 due to their warming effects (Fig. 1). Ground and satellite measurements of concentrations or optical properties of BC and tropospheric O_3 over China, as well as the model estimates of radiative forcing by these two species are summarized. We also review regional and global modeling studies which have investigated climate change driven by BC and tropospheric O_3 in China. Based on the review of previous studies, the key priorities for future research on climatic effects of BC and tropospheric O_3 are highlighted. This review is mainly focused on the studies of BC and tropospheric O_3 by Chinese scientists over the past several years, and the climatic impacts are confined to the impacts of BC and O_3 in the atmosphere within the Chinese territory. Note that China's climate may be affected by BC and O_3 outside China due to complex feedbacks in the climate system.

2. Black carbon and its climatic effects

2.1 Emissions

BC (alternatively referred to as elementary carbon and soot) is released into the atmosphere during the incomplete combustion of fossil fuel, biofuel, and biomass. Emissions of BC in China are large due to its large population, substantial fuel consumption, and often-inefficient combustion conditions, which were reported to be responsible for about 19% of the global BC emission (Qin and Xie, 2012).

Figure 2 shows the spatial distributions of BC emissions. BC emissions were much higher in eastern China than in western China. Western China is typically low in emissions, due to the relatively underdeveloped economy and the small consumption of fossil fuels. Western regions, including Tibet, Xinjiang, Qinghai, Gansu, and Ningxia, cover 42.4% of territory, made up only 3.8%, 4.0%, 4.7% and 5.7% of national BC emissions in 1985, 1995, 2005, and 2009 (Qin and Xie, 2012), respectively. Table 1 summarizes BC emissions in China from different studies. The annual total emission of BC in China after 2006 exceeded 1.79 Tg yr^{-1} (Zhang Q. et al., 2009; Qin and Xie, 2012; Wang et al., 2012). According to Lu et al. (2011), the

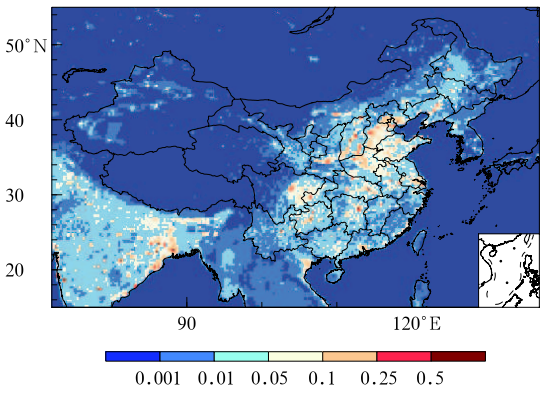

Fig. 2. Spatial distributions of BC emissions (Gg C $grid^{-1}$) at a resolution of 0.1°× 0.1° in 2010. The emissions were compiled by the Emissions Database for Global Atmospheric Research (EDGAR) team and are downloaded from http://edgar.jrc.ec.europa.eu/htap_v2/index.php?SECURE=123.

percentage contributions from sectors of power, industry, residential, transport, and biomass burning to the total BC emission in China were 1.1%, 27.1%, 50.6%, 15.3%, and 5.9%, respectively, in 2010 (Table 1).

Table 1. Summary of BC emissions from different emission sectors in China (units: Gg yr^{-1})

Reference	Year	Power	Industry	Residential	Transport	Biomass burning	Total
Cao et al. (2006)	2000	7.9(0.5%)	543.9(36.3%)	817.6(54.5%)	26.8(1.8%)	103.0(6.9%)	1499.2
Zhang Q. et al. (2009)	2001	38(2.4%)	545(34.2%)	868(54.4%)	143(9.0%)		1595
	2006	36(2.0%)	575(31.8%)	1002(55.3%)	198(10.9%)		1811
Qin and Xie (2011)	2000	6.1(0.5%)	386.0(31.4%)	647.5(52.7%)	121.6(9.9%)	67.3(5.5%)	1228.5
Lu et al. (2011)	1996	12(0.8%)	527(34.6%)	790(51.8%)	92(6.1%)	102(6.7%)	1524
	2000	11(0.9%)	370(29.3%)	639(50.6%)	139(11.0%)	104(8.2%)	1263
	2004	14(0.9%)	437(27.9%)	826(52.6%)	194(12.4%)	98(6.2%)	1569
	2008	19(1.1%)	510(28.6%)	888(49.7%)	259(14.5%)	110(6.1%)	1786
	2010	21(1.1%)	501(27.1%)	936(50.6%)	283(15.3%)	109(5.9%)	1850
Qin and Xie (2012)	1980	1.3(0.1%)	125.4(14.4%)	715.4(82.0%)	25.5(3.0%)	4.3(0.5%)	871.9
	1990	3.7(0.3%)	225.8(18.6%)	899(73.9%)	73.2(6.0%)	14.1(1.2%)	1215.8
	2000	6.1(0.5%)	337.4(28.4%)	647.5(54.6%)	153.1(12.9%)	43.2(3.6%)	1187.3
	2009	11.3(0.6%)	734.6(39.1%)	777.4(41.3%)	241.2(12.8%)	116.6(6.2%)	1881.1
Wang et al. (2012)	2007	50.7(2.6%)	646(33.1%)	988(50.7%)	188(9.6%)	77.7(4.0%)	1957

The value in the brackets is the percentage contribution from an emission sector to total BC emission in China.

2.2 Ground-based measurements of BC concentrations in China

Due to the different instruments used to measure concentrations, BC was also reported as elementary carbon or soot in previous studies. From a measurement stand point, BC mostly refers to aerosol measured with photo-absorption techniques, whereas elementary carbon mostly refers to aerosol measured with thermal/optical techniques. The mass concentrations determined with these two techniques can sometimes be significantly different. For the purpose of this review, we consider BC and elementary carbon to be equivalent in our review and refer the readers to Table 2 for the BC measurement methods used in the studies reviewed below.

Since 1999, carbonaceous aerosols have been measured at numerous locations in China at remote sites (Qu et al., 2006), regionally representative rural sites (Zhang et al., 2005; Gao et al., 2008), and urban sites

Table 2. Summary of BC measurement methods used in the referred studies

Study	Measurement method	EC/BC/soot
Cao et al. (2007)	Samples collected by 47-mm Whatman quartz-fiber filters and analyzed for EC by thermal/optical approach (following IMPROVE_TOR protocol on a DRI model 2001 carbon analyzer)	EC
Cao et al. (2009)	Samples collected by 47-mm Whatman quartz-fiber filters and analyzed for EC by using a Sunset Model 3 OC/EC Analyzer, following thermal/optical transmittance (TOT)	EC
Zhang Q. et al. (2009)	Samples collected by 47-mm Whatman quartz-fiber filters and thermo-chemical analysis for EC used TOR following the IMPROVE protocol	EC
Xu et al. (2009)	Samples from ice cores were filtered through prefired quartz fiber filters and BC on the filters was measured by using the IMPROVE_TOR protocol	Black soot
Han et al. (2011)	IMPROVE_A TOR, STN_thermal optical transmittance (TOT), and chemothermal oxidation (CTO)	EC
Cong et al. (2013)	Analyzed for BC using a DRI model 2001 carbon analyzer following the IMPROVE_A protocol	BC

IMPROVE: Interagency Monitoring of Protected Visual Environments; TOR: thermal optical reflectance; TOT: thermal/optical transmittance; EC: elementary carbon.

in large and mega cities (Xu et al., 2002; Cao et al., 2007; Zhang X. et al., 2008; Cao et al., 2009). Figure 3 presents the measured BC concentrations in 2006 at 18 stations in China (Zhang X. et al., 2008). The average annual mean concentration of BC was 0.35±0.01 μg m^{-3} at the remote background sites of Shangri-la, Zhuzhang, and Akdala, 3.6±0.93 μg m^{-3} at the regional sites of Taiyangshan, Longfengshan, Dunhuang, Lin'an, Jinsha, Lhasa, Nanning, Dalian, Gaolanshan, Shangdianzi, and Zhenbeitai, and 11.2±2.0 μg m^{-3} at the urban sites of Panyu, Zhengzhou, Chengdu, Gucheng, and Xi'an. The highest annual mean BC concentration of 14.2 μg m^{-3} was found at Xi'an in 2006 (Zhang X. et al., 2008). Similar magnitudes of measured BC concentrations were also reported in the study of Cao et al. (2007).

Measured concentrations of BC in China showed strong seasonal variations, with maximum concentrations in winter and minimum values in summer (Cao et al., 2007, 2009; Zhang X. et al., 2008). Cao et al. (2007) showed that the observed BC concentrations averaged over the 14 cities in China were 9.9 μg m^{-3} in winter (6–20 January) and 3.6 μg m^{-3} in summer (3 June–30 July) of 2003. Such seasonal variations can be explained by the largest coal combustion in winter and the largest precipitation associated with the East Asian summer monsoon that washes out BC in summer.

Historical changes in BC are important for understanding the historical changes in climate. Changes in deposition of BC in China were reconstructed by using ice core records (Xu et al., 2009; Cong et al., 2013) or lake sediments (Han et al., 2011). Xu et al. (2009) extracted ice cores from five sites in the Tibetan Plateau and found that the average BC concentrations in ice cores increased from 4.57 ng g^{-1} in 1956 to 12.5 ng g^{-1} in 2006. Han et al. (2011) used a 150-yr (1850–2000) sediment record of Lake Chaohu in Anhui Province and showed that BC concentrations in the sediment exhibited stable low values (below 150000 ng g^{-1}) prior to the late 1970s, and a sharp increase to 450000 ng g^{-1} in the last three decades, corresponding well with the rapid industrialization of China. Cong et al. (2013) reported the variation of BC in sediment of Nam Co Lake in the Tibetan Plateau. From the 1850s to the early 1900s, deposition fluxes of BC to Nam Co Lake were generally constant, which can be considered as background level without significant disturbance from human activities. After the 1900s, BC fluxes showed a gradual and continuous increase, indicating that the influence from anthropogenic sources began in the interior of the Tibetan Plateau. From the 1960s to the early 2000s, the increasing trend of BC deposition flux accelerated significantly. Note that BC in ice core or lake sediment is dependent on BC concentrations in the atmosphere as well as wet and dry deposition of atmospheric BC.

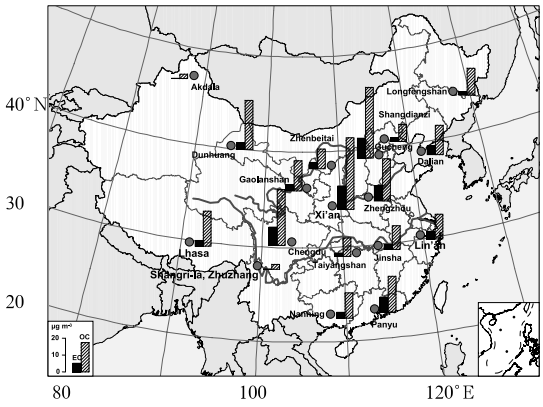

Fig. 3. Locations and annual averaged concentrations of observed BC in 2006. The concentrations at Shangdianzi, Zhenbeitai, Akdala, Shangri-la, and Zhuzhang were from 2004 to 2005. (Source: Fig. 1 of Zhang X. et al. (2008))

As reviewed above, previous measurements of BC were quite limited to BC at the surface. The observations of vertical distribution of BC are needed for the studies of climatic effect of BC, considering that a large fraction of BC particles from biomass burning in South Asia can be transported to the middle troposphere over China in spring of every year (Zhang et al., 2010b). The measurements of size distribution are also essential, because recent observational study indicated that quite a large fraction of BC in China can stay in coarse mode (Wang et al., 2014). Note that the studies of climatic effect of aerosols require long-term measurements, since climate represents multi-year averages of meteorological parameters.

2.3 Optical properties of BC

Aerosol optical depth (AOD) represents light at-

tenuation by aerosols, which is an important parameter that determines the climatic effect of aerosols. Figure 4 shows the annual mean AOD retrieved by Moderate Resolution Imaging Spectrometer (MODIS) that is averaged over 2001–2010. The high AOD values of 0.5–0.9 occurred over a large fraction of eastern China. The AOD values exceeded 0.5 over the heavily polluted northern China, the Sichuan basin, the Yangtze River Delta, and the Pearl River Delta. Such features of AOD were captured by many modeling studies (e.g., Ma et al., 2007; Cui et al., 2009; Zhang et al., 2010a; Lou et al., 2014).

For BC, its unique strong absorption of solar radiation is represented by aerosol absorption optical depth (AAOD), or the non-scattering fraction of AOD. Figure 5 shows the AErosol RObotic NETwork (AERONET) sunphotometer and Ozone Monitoring Instrument (OMI) satellite retrievals of clear-sky AAOD. Measurements from AERONET showed that the AAOD values were in the range of 0.015–0.07, with high values over northern China where concentrations of both BC and mineral dust aerosols were high. On an annual mean basis, AERONET AAOD over Asia (30°–70°N, 100°–160°E) was 0.036, which was much higher than the AAOD of 0.007 over North America (20°–55°N, 130°–70°W) and of 0.015 over Europe (30°–70°N, 15°W–45°E) (Koch et al., 2009). The AAOD values from OMI exhibited high values of exceeding 0.05 over northern China, the Sichuan basin, and the south border of China. Note that both BC and mineral dust aerosols absorb radiation, so AAOD is a useful measure of BC in regions where mineral dust is not a dominant species.

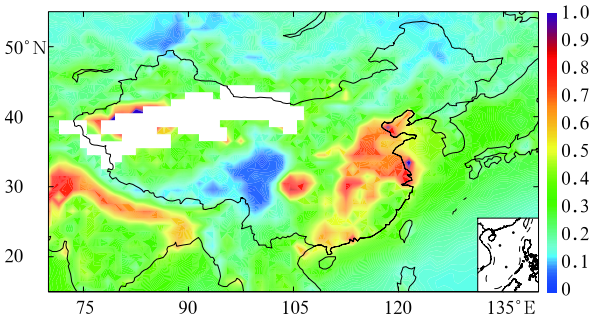

Fig. 4. Annual mean AOD retrieved by Moderate Resolution Imaging Spectrometer (MODIS) that is averaged over 2001–2010. MODIS datasets are level 3 products downloaded from http://ladsweb.nascom.nasa.gov.

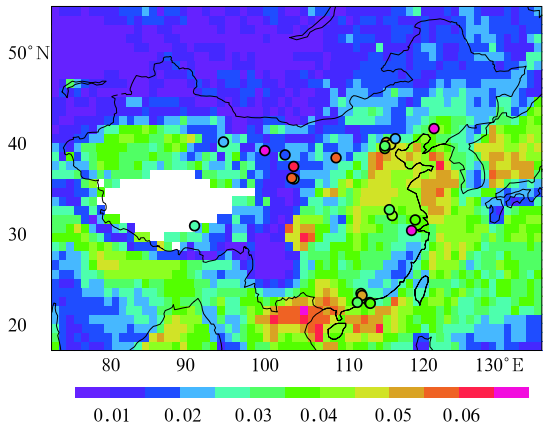

Fig. 5. Aerosol absorption optical depth (AAOD, ×100) from AERONET (at 676 nm, color circles) and OMI (at 500 nm, color shades). AERONET measurements were carried out in different years; the AAOD for a specific site is the average over years with measurements available. The OMI datasets downloaded from http://disc.sci.gsfc.nasa.gov/giovanni are averaged over 2005–2007. The AERONET datasets are downloaded from http://aeronet.gsfc.nasa.gov/cgi-bin/climo_menu_v2_new.

The single scattering albedo (SSA) represents the ratio of aerosol scattering coefficient to extinction coefficient. It is an important optical parameter that determines whether aerosols have a cooling or a warming effect. Over a specific location, SSA is dependent on the mixing of scattering and absorbing aerosol species. Ramanathan et al. (2001) showed that SSA exceeding 0.95 led to a negative aerosol forcing at the top of atmosphere (TOA) and SSA less than 0.85 led to a positive forcing. Bergin et al. (2001) reported that the values of SSA were about 0.81 in polluted northern China. Lee et al. (2007) found that the average of SSA values over China was 0.89±0.04 at 500 nm for 2005. Table 3 summarizes ground-based measurements of SSA in China from the literature. The large differences in SSA can be explained by the differences in shape, size, chemical composition, and hydroscopic growth of aerosol particles.

Qiu and Yang (2008) showed that measured SSA values were the smallest in winter among all seasons.

Table 3. Summary of ground-based measurements of aerosol single scattering albedo in China. The measurements are taken from Liao and Chang (2014)

Location	Period	Single scattering albedo		Reference	Notes on measurements
		λ (nm)	SSA		
Beijing	Jun. 1999		0.81±0.08	Bergin et al. (2001)	Relative humidity < 40%
	1993–2001	550	0.84	Qiu et al. (2004)	
	Jan. 2005	532	0.78±0.11	Müller et al. (2006)	
	2002–2007 spring		0.89	Yu et al. (2009)	Average SSA at wavelengths of 440, 675, 870, and 1020 nm
	summer		0.91		
	autumn		0.87		
	winter		0.86		
	2005–2006	525	0.80±0.09	He et al. (2009)	Relative humidity < 60%
	11 Aug.–6 Sep. 2006	535	0.86±0.07	Garland et al. (2009)	Relative humidity 28±4%
	2001–2004	440	0.9	Xia et al. (2006)	
	2005	550	0.88	Lee et al. (2007)	
	1998–2003	400–1000	0.89	Qiu and Yang (2008)	
Shangdianzi	Sep. 2003–Jan. 2005	525	0.88±0.05	Yan et al. (2008)	Relative humidity < 60%
Xianghe	Sep. 2004–Sep. 2005	441	0.92	Li C. et al. (2007)	
		673	0.92		
		873	0.91		
		1022	0.91		
	Mar. 2005	550	0.81–0.85	Li Z. et al. (2007)	Relative humidity < 36%
	2005	550	0.87	Lee et al. (2007)	
Harbin	1993–2001	550	0.85	Qiu et al. (2004)	
Shenyang	1993–2001	550	0.80	Qiu et al. (2004)	
	2005	550	0.89	Lee et al. (2007)	
	1998–2003	400–1000	0.88	Qiu and Yang (2008)	
Zhengzhou	1993–2001	550	0.85	Qiu et al. (2004)	
	1998–2003	400–1000	0.92	Qiu and Yang (2008)	
Wuqing	Mar. 2009	637	0.82±0.05	Ma et al. (2011)	Dry aerosol
	Jul.–Aug. 2009	637	0.86±0.05		
Xinken	Oct. 2004	532	0.77±0.12	Müller et al. (2006)	
	Oct.–Nov. 2004	550	0.85±0.04	Wendisch et al. (2008)	Dry aerosol
	Oct. 2004	550	0.83±0.05	Cheng et al. (2008)	Relative humidity < 10%
Guangzhou	Oct. 2004	540	0.83	Andreae et al. (2008)	Relative humidity < 45%
Taibei	2005	550	0.83	Lee et al. (2007)	
Shanghai	2005	550	0.87	Lee et al. (2007)	
	1998–2003	400–1000	0.90	Qiu and Yang (2008)	
Wuhan	1998–2003	400–1000	0.94	Qiu and Yang (2008)	
Lin'an	Nov. 1999	530	0.93±0.04	Xu et al. (2002)	Relative humidity < 40%
Shouxian	May–Dec. 2008	550	0.92	Fan et al. (2010)	Relative humidity < 40%
Dunhuang	1998–2000	550	0.90	Kim et al. (2004)	
Yinchuan	1998–2000	500	0.91	Kim et al. (2004)	
	Oct. 2003–Aug. 2004	500	0.83–0.95	Liu et al. (2008)	
Yulin	Apr. 2001		0.95±0.05	Xu et al. (2004)	Relative humidity 35±21%
Ürümqi	1993–2001	550	0.84	Qiu et al. (2004)	
	1998–2003	400–1000	0.89	Qiu and Yang (2008)	
Lanzhou	1993–2001	550	0.81	Qiu et al. (2004)	
	2005	550	0.89	Lee et al. (2007)	
	1998–2003	400–1000	0.85	Qiu and Yang (2008)	
Chengdu	1998–2003	400–1000	0.90	Qiu and Yang (2008)	

The increase in BC emission might have led to the decrease in SSA in Beijing during 1993–2001 (Qiu et al., 2004). Lyapustin et al. (2011) examined AOD values in Beijing from both the AERONET measurements and the MODIS retrievals, and reported an increasing trend in SSA in Beijing during 2007–2010 relative

to the previous 5 years. Particularly, as dust particles were mixed with anthropogenic aerosols during the transport, SSA values generally showed increases, because the retrieved SSA of dust ranged from 0.92 (at 0.44 μm) to 0.97 (at 1.02 μm) and the SSA of anthropogenic aerosols ranged from 0.89±0.04 (at 0.44 μm) to 0.83±0.05 (at 1.02 μm) (Xia et al., 2005). Cao et al. (2014) also reported that SSA increased during dust events in Beijing in 2005.

2.4 Radiative forcing of BC in China

Table 4 summarizes the estimated radiative forcing (RF) of BC over China, including direct radiative forcing (DRF), first indirect radiative forcing (FIRF), and semi-direct radiative forcing. The DRF reviewed in this work refers to an instantaneous change in net (downward minus upward) radiative flux (shortwave plus longwave, in W m^{-2}) due to an imposed change in concentration of a chemical species (i.e., BC in this section and O_3 in Section 3.3). The semi-direct effect of BC is the difference in cloud forcing with and without the impact of BC on SSA of cloud droplet (Zhuang et al., 2010a), and the FIRF of BC is the change in cloud forcing with and without the impacts of BC on effective radius of cloud droplets (Zhuang et al., 2013). The RF of BC is usually defined in terms of change in net radiative flux at the TOA or at the surface.

The DRF of BC is always positive at the TOA and negative at the surface, with the spatial distribution of DRF at the TOA similar to that of DRF at the surface. Chung and Seinfeld (2005), by using a global climate model with online simulation of BC, reported that the present-day maximum TOA all-sky BC DRF over eastern China was about 5–6 W m^{-2} on an annual mean basis. Zhang H. et al. (2008), by using the global aerosol dataset in a radiative transfer model, showed that the TOA clear-sky BC DRF over eastern China reached 3.2 and 4.0 W m^{-2} in winter and summer, respectively. Wu et al. (2008) simulated by using the Regional Climate Chemistry Modeling System (RegCCMs) found that BC DRF values were stronger in southern China than in northern China during this period; the all-sky BC DRF was 0.64 W m^{-2} at the TOA and –1.69 W m^{-2} at the surface over northern China (32°–50°N, 105°–120°E), while it was 1.55 W m^{-2} at the TOA and –3.10 W m^{-2} at the surface over southern China (22°–30°N, 100°–120°E). Zhang H. et al. (2009) and Wang et al. (2009) estimated the DRF of BC by using the global Community Atmosphere Model Version 3 (CAM3). Under all-sky conditions, the present-day annual mean BC DRF over eastern China was simulated to be 2.5 W m^{-2} at the TOA and –3.2 W m^{-2} at the surface. Zhuang et al. (2010b) estimated that the annual mean BC DRF values at TOA were 1.02 W m^{-2} for clear skies and 0.75 W m^{-2} for all skies over China (25°–45°N, 100°–130°E) in 2006. Zhuang et al. (2013) showed that the annual mean BC DRF over China (20°–50°N, 100°–130°E) was 0.81 W m^{-2} at the TOA in 2006, and the strongest TOA BC DRF was 6.0 W m^{-2} over the Sichuan basin. Among the BC DRF estimates for China, the values obtained by Zhang et al. (2012) were relatively small; the simulated annual mean TOA BC DRF exhibited maximum value of 1.0 W m^{-2} under all-sky and of 0.8 W m^{-2} under clear-sky conditions. The low bias in simulated BC column burden might have led to the small BC forcing in Zhang et al. (2012).

BC can act as cloud condensation nuclei (CCN) and influence cloud albedo, exerting a negative FIRF at the TOA. Zhuang et al. (2009) reported that the regional average (20°–50°N, 90°–120°E) of TOA BC FIRF was –0.39 W m^{-2} in January and –1.18 W m^{-2} in July 2003. Zhuang et al. (2013) estimated that the TOA FIRF of BC was –0.95 W m^{-2} over China (20°–50°N, 100°–130°E), which was larger than its DRF, leading to a net RF of BC of –0.15 W m^{-2} at the TOA for 2006.

BC can burn clouds through heating the ambient air around and clouds (semi-direct effect of BC), which reduces cloud cover and allows more shortwave radiative fluxes to reach the surface. Zhuang et al. (2010a) showed that the average semi-direct RF values over eastern China (20°–50°N, 100°–130°E) were 0.04, 0.10, 0.09, and 0.06 W m^{-2} at the TOA in January, April, July, and October 2003, respectively.

As shown in Table 4, the simulated regional mean DRF values are in the range of 0.75–2.5 W m^{-2}, which are significant as compared to the global mean radia-

Table 4. Summary of estimates of radiative forcing of BC in China

Reference	Model	Region	Time	Aerosol effects	TOA /SRF	Clear-sky radiative forcing (W m^{-2})		All-sky radiative forcing (W m^{-2})	
						Mean	Max	Mean	Max
Chung et al. (2005)	GISS	East China	2000	DRF	TOA				+6.0
		Southern China (22°–30°N, 100°–120°E)			TOA			+1.55	
					SRF			–3.10	
Wu et al. (2008)	RegCM3	Northern China (32°–50°N, 105°–120°E)	1993–2003	DRF	TOA			+0.64	
					SRF			–1.69	
		China (32°–50°N, 105°–120°E)			TOA		+2.5	+1.10	
					SRF			–2.40	
Zhang H. et al. (2008)	GADS and radiative trasnfer model	Eastern China	Winter	DRF	TOA		+3.2		
					SRF		–11.0		
			Summer		TOA		+4.0		
					SRF		–11.0		
Zhang H. et al. (2009)	CAM3	Eastern China	Present-day	DRF	TOA		+1.0		+2.5
Wang et al. (2009)	CAM3	Eastern China	2000	DRF	TOA			+2.5	
					SRF			–3.2	
Zhuang et al. (2009)	RegCCMs	China (20°–50°N, 90°–120°E)	Jan. 2003	FIRF	TOA			–0.39	
					SRF			–0.39	
			Jul. 2003		TOA			–1.18	
					SRF			–1.19	
			2003		TOA			+0.07	
Zhuang et al. (2010a)	RegCM3	China (20°–50°N, 100°–130°E)	Jan.	Semi	TOA			+0.04	
			Apr.		TOA			+0.10	
			Jul.		TOA			+0.09	
			Oct.		TOA			+0.06	
Zhuang et al. (2010b)	RegCCMs & WRFchem	China (25°–45°N, 100°–130°E)	2006	DRF	TOA	+1.02	+7.0	+0.75	+5.5
					SRF	–3.18		–2.02	
Zhang et al. (2012)	AGCM	East China	Present-day	DRF	TOA		+0.8		+1.0
Zhuang et al. (2013)	RegCCMs	China (20°–50°N, 100°–130°E)	2006	DRF	TOA			+0.81	+6.0
				FIRF				–0.95	–6.5
Zhuang et al. (2014)	Observed	Nanjing (32.05°N, 118.78°E)	22 Apr. 2011–21 Apr. 2012	DRF	TOA			+0.45	
					SRF			–7.9	

DRF: direct radiative forcing of BC. FIRF: first indirect radiative forcing of BC. SRF: radiative forcing at the surface. TOA: radiative forcing at the top of atmosphere. Semi: semi-direct radiative forcing of BC.

tive forcing values of BC, tropospheric O_3, and CO_2. IPCC (2013) reported that between 1750 and 2011, the global and annual mean RF values of BC, tropospheric O_3, and CO_2 were 0.40 (0.05–0.80) W m^{-2}, 0.40 (0.20–0.60) W m^{-2}, and 1.82 (1.63–2.01) W m^{-2}, respectively. Recently, Bond et al. (2013) reported the annual mean BC DRF exceeded 5 W m^{-2} over a large fraction of eastern China, which further underscores the importance of BC in regional warming of climate. However, few studies have examined semi-direct and indirect effect RF of BC; the RF values of semi-direct and indirect effect of BC have large uncertainties and

are subject to further studies.

2.5 Climatic effect of BC

Increases in BC concentrations in the atmosphere were simulated to lead to a warming over China. Chang et al. (2009) found by using a coupled global aerosol-climate model that the direct effect of BC increased the surface air temperature averaged over eastern China (20°–50°N, 100°–130°E) by 0.62℃ over 1950–2000. Jiang Y. et al. (2013) used the NCAR Community Atmospheric Model version5 (CAM5) and found that during 1850–2000, the direct and indirect effects of BC led to changes in surface air temperature by –0.6 to 0.3 K over East China (20°–45°N, 105°–122.5°E). Guo et al. (2013) reported by using the United Kingdom High-Resolution Global Environment Model (HiGAm) that BC direct effect changed the monthly and regional mean surface air temperature over East Asia (20°–45°N, 100°–122°E) by –0.4 to 0.1 K during April–September. The simulated negative changes in temperature by BC indicated the complex BC-cloud feedbacks.

BC affects the large-scale circulation and hydrological cycle by heating the air and hence altering the regional atmospheric stability. Menon et al. (2002) considered the direct effect of BC in the Goddard Institute for Space Studies (GISS) global climate model and reported that the radiative effect of BC in China and India led to the observed "northern droughts and southern floods" in China over the past several decades. Chang et al. (2009) used a coupled global aerosol-climate model and found that the direct effect of BC increased precipitation over 1950–2000 by 0.07 mm day^{-1} as precipitation was averaged over eastern China (20°–50°N, 100°–130°E). Zhuang et al. (2013) showed by using the RegCCMs that the combined effect of BC (semi-direct plus indirect effect) led to regional mean change in precipitation by –0.09 mm day^{-1} (or –7.4%) over eastern China (20°–50°N, 100°–130°E) for 2006. Jiang Y. et al. (2013) considered both direct and indirect effects of BC in the NCAR CAM 5 and reported that BC led to summertime change in precipitation by –0.08 mm day^{-1} from 1850 to 2000 as precipitation was averaged over East China (20°–45°N, 105°–122.5°E).

BC also contributes to the retreat of the glaciers over the Himalayas (Ming et al., 2008; Xu et al., 2009; Menon et al., 2010; Kopacz et al., 2011; Wang Z. et al., 2011; Wang X. et al., 2014). As BC is deposited over snow and sea ice, it significantly enhances solar absorption by snow and ice. Ming et al. (2008) estimated radiative forcing by using BC retrieved from a 40-m shallow ice core from the East Rongbuk Glacier in the high Himalayas. They reported a local radiative forcing of as large as 5.0 W m^{-2} by BC deposited in the glacier, suggesting that BC in the atmosphere over the Himalayas and consequently in the glaciers cannot be neglected when assessing the dual warming effects on glacier melting. Menon et al. (2010) simulated by using the NASA GISS climate model (ModelE) with on-line aerosol chemistry that about 0.9% of snow/ice cover decreases over the Himalayas during 1990–2000 was caused by direct effect, indirect effect, and deposition of BC aerosol. Wang Z. et al. (2011) simulated by using the BCC_AGCM that the regional mean radiative forcing due to BC deposited on snow/ice reached 2.8 W m^{-2} over the Tibetan Plateau and led to increases in annual mean temperature by 1.6 K in that region.

Modeling studies reviewed above show large uncertainties, either in simulated radiative forcing or in simulated climate responses, although the regional and global climate models start to have the capabilities to simulate BC-radiation and BC-cloud interactions. The uncertainties arise in part from emissions inventories, representation of concentrations, vertical profiles, mixing states, and optical properties of BC. The representation of the aging of BC and the role of BC as cloud condensation nuclei remains to be the most difficult challenges in simulation of climatic effect of BC (IPCC, 2013). Nationwide long-term measurements of aerosol concentrations, aerosol optical properties, and cloud properties in China are called for to constrain model simulations.

3. Ozone and its climatic effects

3.1 Emission of O_3 precursors

The most important O_3 precursors in the atmosphere include NO_x, CO, and volatile organic compounds (VOCs). Motor vehicle exhaust, industrial

emissions, and chemical solvents are the major anthropogenic sources of these chemicals. As an example, Table 5 summarizes the annual emissions of NO_x, CO, and NMVOCs in eastern China (20°–50°N, 110°–126°E), which are based on David Streets' 2006 emission inventory (http://mic.greenresource.cn/intex-b 2006) (Zhang Q. et al., 2009). Note that tropospheric O_3 has a lifetime of about 3 weeks (Liao and Seinfeld, 2005; Stevenson et al., 2006) and therefore a large fraction of O_3 in China can be attributed to background O_3 and anthropogenic emissions from foreign countries (Wang Y. et al., 2011).

3.2 Simulated and observed concentrations of tropospheric O_3

Figure 6 shows the distributions of seasonal mean surface-layer concentrations of O_3 simulated for 2006 in the study of Lou et al. (2014) by using a global chemical transport model. Simulated concentrations of O_3 in eastern China are the lowest in DJF because

Table 5. Annual emissions of ozone precursors in eastern China (20°–50°N, 110°–126°E)

Species	Eastern China
NO_x (Tg N yr^{-1})	
Aircraft	0.01
Anthropogenic	4.88
Biomass burning	0.01
Fertilizer	0.09
Lightning	0.16
Soil	0.16
Total	5.32
CO (Tg CO yr^{-1})	
Anthropogenic	130.89
Biomass burning	1.11
Total	132.00
NMVOCs (Tg C yr^{-1})	
Anthropogenic	6.71
Biomass burning	0.05
Biogenic	9.50
Total	16.26

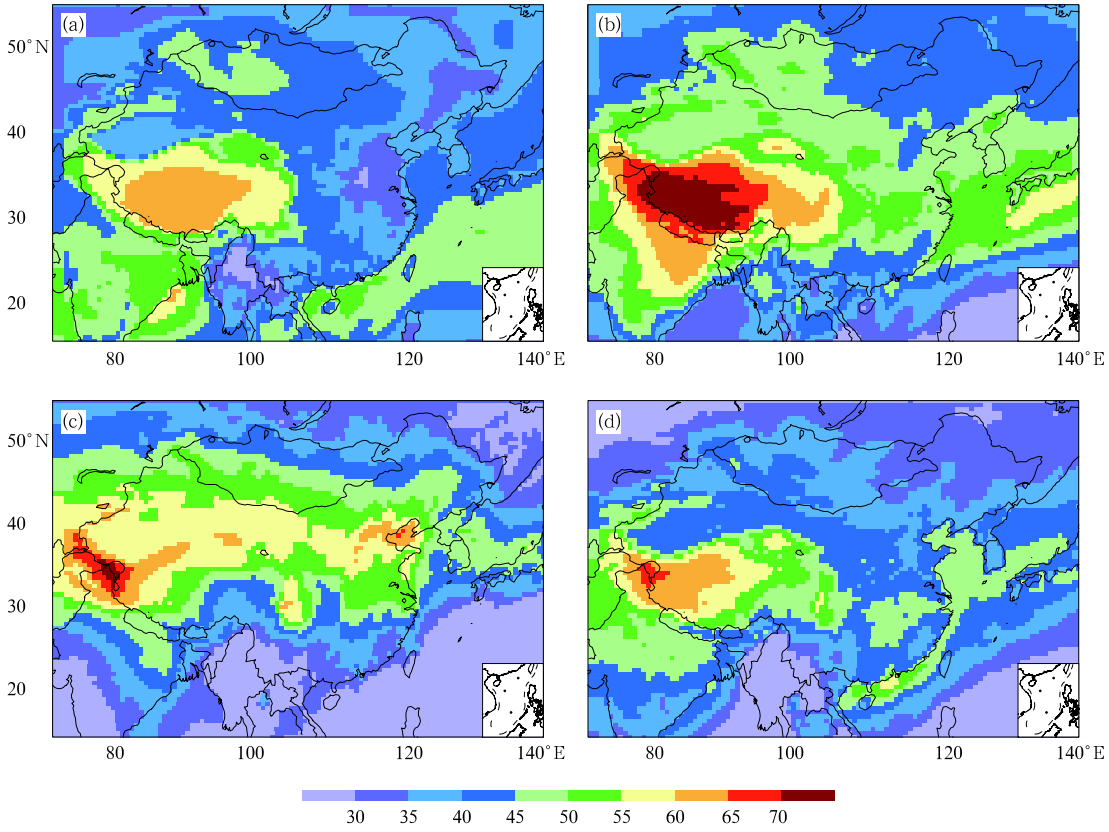

Fig. 6. Simulated seasonal mean surface-layer concentrations (ppbv) of O_3 for 2006. (a) DJF (December–January–February), (b) MAM (March–April–May), (c) JJA (June–July–August), and (d) SON (September–October–November), respectively. (Remade from Fig. 2 of Lou et al. (2014))

of the weak photochemistry as a result of weak solar radiation in this season. Concentrations of O_3 in eastern China in MAM and SON are in the ranges of 40–55 and 35–50 ppbv, respectively. The maximum O_3 concentrations over eastern China are simulated to be 60–75 ppbv in JJA. Note that the high O_3 concentrations of exceeding 70 ppbv over the Tibetan Plateau in MAM result from the transport of O_3 from the stratosphere to troposphere (Wild and Akimoto, 2001).

Table 6 compiles the ground-based measurements of O_3 in China from the literature. During July–September of 2001–2006, the average measured O_3 concentrations at 6 urban sites in Beijing was 26.6±2.8 ppbv (Tang et al., 2009). At remote sites (Fenghuanshan (40.5°N, 124°E), Waliguan in the Qinghai-Tibetan Plateau (36.3°N, 100.9°E), Lin'an (31.3°N, 120.4°E), and Longfengshan Mountain (44.7°N, 127.6°E)), O_3 concentrations were generally in the range of 20–60 ppbv (Yan et al., 1997, 2003; Wang et al., 2004; Takami et al., 2006; Wang et al., 2006). The background O_3 concentrations are relatively higher in western China as a result of the transport of O_3 from the stratosphere. For example, concentrations at Waliguan (36.3°N, 100.9°E) were in the range of 40–60 ppbv, which were higher than the measured values at other background stations. With respect to the long-term trend of O_3, surface concentrations measured in Lin'an, a background station in eastern China, showed that the monthly highest 5% O_3 concentrations increased over 1991–2006 (Xu et al., 2008).

Estimating of the climatic effect of tropospheric O_3 requires knowledge of not only surface concentrations but also vertical distributions and column burdens. Ozonesonde datasets were available at only a number of sites in China. Based on 810 vertical profiles of O_3 measured by aircraft in different seasons of 1995–2005, Ding et al. (2008) showed that the average mixing ratio of O_3 in Beijing increased from about 40 ppbv at the ground to about 50 ppbv at 2-km altitude. Satellite measurements are useful for analyses of the distributions and seasonal variations of tropospheric column O_3 concentration over China because of the excellent spatial and temporal coverage. Liu et al. (2006) presented the first directly retrieved global distribution of tropospheric column O_3 from Global Ozone Monitoring Experiment (GOME) ultraviolet measurements from December 1996 to November 1997. The retrieved columns clearly showed changes owing to convection, biomass burning, stratospheric influence, pollution, and transport. By using measurements from the Infrared Atmospheric Sounding Interferometer (IASI) instrument aboard the European Metop-A satellite (launched in October 2006), Dufour et al. (2010) showed that the maximum O_3 occurs in late spring and early summer (May–June) in Beijing. Wang Y. et al. (2011) examined the month to month variation of mean tropospheric O_3 column from Tropospheric Emission Spectrometer (TES) for eastern (east of 110°E) and western (west of 110°E) China. TES retrievals suggest that column burden of tropospheric ozone over both eastern and western China has a maximum in late spring/early summer and minimum in winter. Although biogenic emissions, temperature, and radiation are the highest in southeastern and southwestern China in July, O_3 concentrations in those regions are generally low in summer because of the summer monsoon circulation that brings clean air from the oceans. Zhang et al. (2014) reported that the retrieved tropospheric O_3 column concentration from OMI averaged over China and from 2010–2013 was 34.0 DU.

3.3 Radiative forcing of tropospheric O_3

Tropospheric O_3 exerts radiative forcing at both longwave and shortwave spectral bands. Few studies have examined the RF by tropospheric O_3 over China. By using a coupled regional chemistry-climate model (RegCM2), Wang et al. (2005) showed that tropospheric O_3 had a shortwave forcing of 0.19 W m^{-2} and a longwave forcing of 0.46 W m^{-2} at the tropopause. They reported that the normalized net radiative forcing over China was 0.02 W m^{-2} DU^{-1}, lower than the global mean values of 0.03–0.05 W m^{-2} DU^{-1} reported in the literature. By using the IPCC AR5 emissions inventories, Chang et al. (2009) reported that the anthropogenic radiative forcing by tropospheric O_3 averaged over eastern China (18°–45°N,

Table 6. Summary of ground measurements of ozone in China

Location	Period		Mixing ratio (ppbv)	Reference
Beijing (39.9°N, 116.5°E)	1995–2005		40	Ding et al. (2008)
	Jul.–Sep. of 2001–2006		26.6±2.8	Tang et al. (2009)
	20 Jun.–16 Sep. 2007		36.2–58.2	Xu et al. (2011)
Miyun (40.5°N, 116.8°E)	2005–2007	Spring	50–55	Wang Y. et al. (2011)
		Summer	85 (Jun.)	
		Autumn	65 (Sep.)	
		Winter	50–55	
Shangdianzi (40.7°N, 117.1°E)	2004–2006	Spring	35.0–41.4	Lin et al. (2008)
		Summer	30.9–46.5	
		Autumn	19.4–34.7	
		Winter	17.7–27.0	
	Sep.–Dec. 2003		26.8±13.9	Meng et al. (2009)
	Jan.–Dec. 2004		30.1±21.0	
	Jan.–Dec. 2005		32.8±19.1	
	Jan.–Dec. 2006		30.9±19.8	
Nanjing (32.0°N, 118.5°E)	Jan. 2000–Feb. 2003	Spring	27.0	Tu et al. (2007)
		Summer	22.8	
		Autumn	18.4	
		Winter	14.1	
Qingdao (36.5°N, 121°E)	24 Feb.–15 Mar. 2002		26.6	Takami et al. (2006)
	16–28 Feb. 2001		23.5	
	15–28 Jan. 2000		35.9	
Qingdao (36.1°N, 120.5°E)	Dec. 1994		23	Li et al. (1999)
	Jun. 1995		35	
Fenghuanshan (40.5°N, 124°E)	16 Feb.–2 Mar. 2001		30.2	Takami et al. (2006)
	13–25 Jan. 2000		32.2	
Waliguan (36.3°N, 100.9°E)	20 Apr.–23 May 2003	Spring	58±9	Wang et al. (2006)
	15 Jul.–16 Aug. 2003	Summer	54±11	
	Aug. 1994–Jul. 1995	Spring	52.2±4.21	Yan et al. (1997)
		Summer	60.9±6.87	
		Autumn	42.1±4.16	
		Winter	42.4±2.73	
Lin'an (31.3°N, 120.4°E)	Dec. 1999		32	Yan et al. (2003)
	Jun. 2000		40	
	Aug. 1994–Jul. 1995	Spring	37.3±5.89	Yan et al. (1997)
		Summer	32.9±7.14	
		Autumn	39.84±6.76	
		Winter	36.9±9.08	
Changshu (30.3°N, 119.4°E)	Jun. 2000		45	Yan et al. (2003)
	Dec. 1999		22	
Waliguan (36.3°N, 100.9°E)	Sep. 1999–Jun. 2001		44.9	Carmichael et al. (2003)
Lin'an (30.3°N, 119.7°E)			38.3	
Shangdianzhi (40.7°N, 117.1°E)			38.0	
Cape D'Aequier (22.2°N, 114.3°E)			34.9	
Longfengshan Mountain (44.7°N, 127.6°E)	Aug. 1994–Jul. 1995	Spring		Yan et al. (1997)
		Summer		
		Autumn		
		Winter		

95°–125°E) was 0.53 W m^{-2} at the tropopause.

3.4 Simulated climatic effect of tropospheric O_3

Several studies examined climate responses to RF of tropospheric O_3 in China. Wang et al. (2004) used a coupled regional chemistry-climate model based on RegCM2 to simulate the concentrations and climatic effect of tropospheric O_3 in China. They reported that the monthly mean column burden of O_3 was about 30 DU and led to changes in surface air temperature by –0.8 to 0.8 K over eastern China. The negative changes in temperature were mainly associated with the feedback of clouds. Based on the transient climate simulations of the GISS ModelE, Hansen et al. (2007) predicted that the increases in surface air temperature by tropospheric O_3 were up to 0.5 K over eastern China from 1900 to 2003. On the basis of a global coupled chemistry-climate simulation, Chang et al. (2009) reported that the warming by tropospheric O_3 was 0.43 K in eastern China over 1950–2000.

The large changes in simulated surface air temperature reviewed above underscore the importance of considering O_3 in policies for mitigating global warming. It should be noted that many previous studies on regional climate changes in China did not account for the role of tropospheric O_3, which would lead to low biases in simulated warming in China.

4. Mitigation of climate warming by reductions in black carbon and O_3 in China

Due to the warming effect of BC and tropospheric O_3 as reviewed above, reductions in short-lived BC and tropospheric O_3 have been proposed as a complementary strategy to reductions in greenhouse gases. Recent studies started to identify approaches to mitigate both air pollution and global warming by reducing concentrations of short-lived species such as tropospheric O_3 and BC (UNEP, 2011; Shindell et al., 2012; Bond et al., 2013; Liao and Chang, 2014; Zhang et al., 2014). BC and OC are always co-emitted, but in different proportions from different emission sources. BC is also co-emitted with other scattering aerosols such as sulfate from fossil fuel burning. As a result, the effect of BC mitigation depends on how BC and co-emitted aerosol species affect cloud properties (cloud albedo, cloud amount, and cloud lifetime) and hence cloud radiative forcing. If such a perturbation were to result in a reduction in TOA cloud cooling, the amount of BC reduction would oppose the amount by which the TOA direct BC heating is also reduced. For example, Chen et al. (2010) considered two present-day mitigation scenarios: 50% reduction of primary BC/OC mass and number emissions from fossil fuel combustion (referred to as HF), and 50% reduction of primary BC/OC mass and number emissions from all primary carbonaceous sources (fossil fuel, domestic biofuel, and biomass burning) (referred to as HC). The global mean TOA changes in radiative forcing for the two scenarios, relative to present day, were calculated to be 0.13±0.33 W m^{-2} (HF) and 0.31±0.33 W m^{-2} (HC), indicating the large uncertainty in the net effect of some BC control measures on global warming.

Few studies have examined the effect of reductions in O_3 on global warming. As a short-lived species with lifetime of about 3 weeks (Liao and Seinfeld, 2005; Stevenson et al., 2006), a large fraction of O_3 in China can be attributed to background O_3 and anthropogenic emissions from foreign countries. Wang Y. et al. (2011) used the global chemical transport model GEOS-Chem to identify contributions of emissions from various source types (natural and anthropogenic) and regions (domestic and foreign) to the spatial distribution and seasonality of tropospheric O_3 in China. Assuming that total O_3 is the sum of total background O_3 (TBO; simulated with global natural emissions as well as anthropogenic emissions outside China) and China pollution O_3 (CPO; O_3 formation from anthropogenic emissions in China), the annual mean TBO over China was calculated to be 44.1 ppbv, with maximum value of 50.7 ppbv in MAM and minimum value of 40.9 ppbv in JJA, accounting for 93% and 81% of total surface O_3 in these seasons, respectively. Annual mean CPO was calculated to be 5.4 ppbv, ranging from 1.4 ppbv in DJF to 9.9 ppbv in JJA. Average over China, CPO contributed about 20% of total O_3 in JJA. These model results indicate that domestic reductions in O_3 through controlling O_3 pre-

cursors (such as NO_x, CO, and NMVOCs) may not be helpful for regional climate; it is important to establish emission control collaboration to achieve mutual benefits among different countries/regions.

Noted that while BC and O_3 affect the regional climate, climate change can affect their distributions and concentrations by altering natural emissions, chemical reactions, transport, and deposition (Liao et al., 2006; Jiang H. et al., 2013; Qu et al., 2013; Wang et al., 2013). Such chemistry-aerosol-climate feedbacks need to be accounted for in policies for future emission reductions.

5. Science needs for reductions of short-lived greenhouse species

As presented in sections above, important advances have been made during the past decade in understanding concentrations and distributions of BC and tropospheric O_3 and their roles in climate change in China. Emissions inventories of tropospheric O_3 and aerosol precursors as well as aerosols have become available for China domain, which allow one to simulate concentrations of BC and tropospheric O_3 and estimate their climatic effects by using numerical models. Increasing availability of ground-based measurements and satellite measurements of short-lived species and their optical properties as well as cloud properties has provided datasets to constrain the simulated climatic effects of aerosols and tropospheric O_3. However, estimates of the net effect of BC and O_3 control measures on global warming are still subject to large uncertainties. The fundamental science needs pertaining to reductions in short-lived species to mitigate global warming are summarized in Fig. 7 and described below.

(1) Quantification of emissions of BC and O_3 precursors from different sectors in China, which are required for making plans of control measures. It is also important to quantify all the chemical species that are co-emitted with BC or O_3 precursors can influence concentrations of both long-lived greenhouse gases and short-lived species. Such information will be helpful for estimating the net radiative forcing of a specific BC or O_3 control measure.

(2) Nationwide long-term measurements of size-

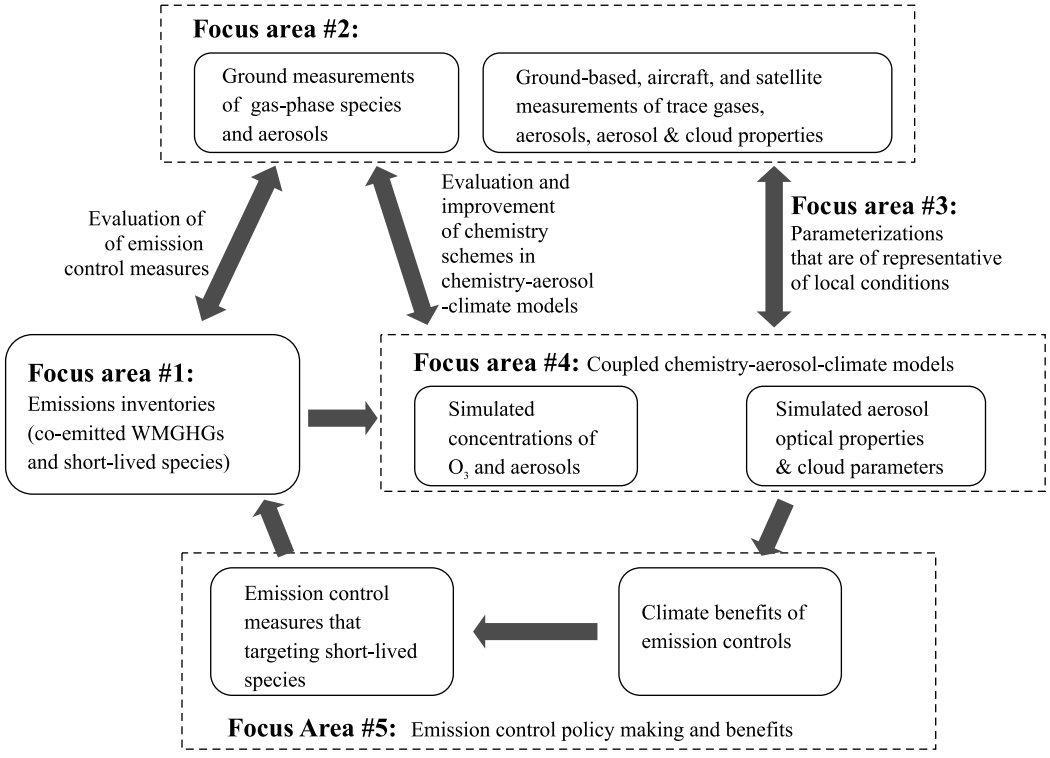

Fig. 7. Fundamental science needs pertaining to reductions in short-lived species to mitigate global warming.

resolved mass concentrations of BC and other aerosol species as well as number concentrations of aerosols. Since previous measurements (measurements at urban sites for short time periods) were mostly designed for air quality studies, nationwide long-term measurements are especially important for climate studies and need coordinated funding support. With fairly good funding support, satellite measurements have excellent spatial and temporal coverage, which are also useful for analyses of the physical/chemical/optical characteristics of O_3 and aerosols. These measurements are necessary for evaluation of emission inventories, development of chemistry-aerosol-climate models, and the assessment of the effect of emission reduction measures (Wang et al., 2012; Xu et al., 2013). Better understanding of BC and tropospheric O_3 also requires satellite measurements of fires. One of the largest uncertainties with the fire observations is in estimating the actual amount of BC and O_3 precursors such as NO_x that are emitted.

(3) Improving the understanding of aerosol-cloud interactions. How chemical species co-emitted with BC influence clouds is one of the most difficult challenges, because the microphysical processes involved are very complex. Although the direct radiative effect of BC has been shown to be a strong warming, the semi-direct and indirect effects of BC have large uncertainties either with sign and magnitude. Considering that aerosol-cloud interactions have the largest uncertainties among the drivers of climate change (IPCC, 2013), quantification of aerosol-cloud interactions is critical for assessing the benefits of emission control measures.

(4) Continuous development of fully coupled chemistry-aerosol-climate models. As reported by IPCC (2013), a large fraction of climate models can simulate chemistry and transport of tropospheric O_3 and aerosols, but few of them have fully coupled meteorology-aerosol-cloud-radiative forcing feedbacks, especially with the consideration of all major anthropogenic and natural aerosol species and the radiative effects of aerosols on distributions and concentrations of chemical species.

(5) Through atmospheric transport, pollutants can be carried from one location to another. Therefore, how different countries/regions are accountable for the emissions and how they can establish emission control collaboration to achieve mutual benefits are very important questions. These issues are relatively less studied in current literature and remain an important bottleneck affecting the effectiveness of emission control.

REFERENCES

Andreae, M. O., O. Schmid, H. Yang, et al., 2008: Optical properties and chemical composition of the atmospheric aerosol in urban Guangzhou, China. *Atmos. Environ.*, **42**, 6335–6350.

Bergin, M. H., G. R. Cass, J. Xu, et al., 2001: Aerosol radiative, physical, and chemical properties in Beijing during June 1999. *J. Geophys. Res.*, **106**, 17969–17980.

Bond, T. C., S. J. Doherty, D. W. Fahey, et al., 2013: Bounding the role of black carbon in the climate system: A scientific assessment. *J. Geophys. Res.*, **118**, 5380–5552.

Cao, G. L., X. Y. Zhang, and F. C. Zheng, 2006: Inventory of black carbon and organic carbon emissions from China. *Atmos. Environ.*, **40**, 6516–6527.

Cao, J. J., S. C. Lee, J. C. Chow, et al., 2007: Spatial and seasonal distributions of carbonaceous aerosols over China. *J. Geophys. Res.*, **112**, D22s11, doi: 10.1029/2006JD008205.

Cao, J. J., Z. X. Shen, J. C. Chow, et al., 2009: Seasonal variations and sources of mass and chemical composition for PM_{10} aerosol in Hangzhou, China. *Particuology*, **7**, 161–168.

Cao, C. X., S. Zheng, and R. P. Singh, 2014: Characteristics of aerosol optical properties and meteorological parameters during three major dust events (2005–2010) over Beijing, China. *Atmos. Res.*, **150**, 129–142.

Carmichael, G. R., M. Ferm, N. Thongboonchoo, et al., 2003: Measurements of sulfur dioxide, ozone and ammonia concentrations in Asia, Africa, and South America using passive samplers. *Atmos. Environ.*, **37**, 1293–1308.

Chang Wenyuan, Liao Hong, and Wang Huijun, 2009: Climate responses to direct radiative forcing of anthropogenic aerosols, tropospheric ozone, and long-

lived greenhouse gases in eastern China over 1951–2000. *Adv. Atmos. Sci.*, **26**, 748–762.

Chen, W.-T., Y. H. Lee, P. J. Adams, et al., 2010: Will black carbon mitigation dampen aerosol indirect forcing? *Geophys. Res. Lett.*, **37**, L09801, doi: 10.1029/2010GL042886.

Cheng, Y. F., A. Wiedensohler, H. Eichler, et al., 2008: Aerosol optical properties and related chemical apportionment at Xinken in Pearl River Delta of China. *Atmos. Environ.*, **42**, 6351–6372.

Chung, S. H., and J. H. Seinfeld, 2005: Climate response of direct radiative forcing of anthropogenic black carbon. *J. Geophys. Res.*, **110**, doi: 10.1029/2004JD005441.

Cong, Z. Y., S. C. Kang, S. P. Gao, et al., 2013: Historical trends of atmospheric black carbon on Tibetan Plateau as reconstructed from a 150-yr lake sediment record. *Environ. Sci. Technol.*, **47**, 2579–2586.

Cui Zhenlei, Zhang Hua, and Yin Yan, 2009: A modeling study with MATCH on the aerosol optical depth distribution over China in 2006. *Remote Sensing Technology and Application*, **24**, 197–203. (in Chinese)

Ding, A. J., T. Wang, V. Thouret, et al., 2008: Tropospheric ozone climatology over Beijing: Analysis of aircraft data from the MOZAIC program. *Atmos. Chem. Phy.*, **8**, 1–13.

Dufour, G., M. Eremenko, J. Orphal, et al., 2010: IASI observations of seasonal and day-to-day variations of tropospheric ozone over three highly populated areas of China: Beijing, Shanghai, and Hong Kong. *Atmos. Chem. Phy.*, **10**, 3787–3801.

Fan Xuehua, Cheng Hongbin, Xia Xiangao, et al., 2010: Aerosol optical properties from the atmospheric radiation measurement mobile facility at Shouxian, China. *J. Geophys. Res.*, **115**, D00K33, doi: 10.1029/2010JD014650.

Gao Runxiang, Niu Shengjie, Zhang Hua, et al., 2008: An observational study of black carbon aerosol in Northwest China in the spring of 2006. *J. Nanjing Inst. Meteor.*, **31**, 655–661. (in Chinese)

Garland, R. M., O. Schmid, A. Nowak, et al., 2009: Aerosol optical properties observed during Campaign of Air Quality Research in Beijing 2006 (CAREBeijing-2006): Characteristic differences between the inflow and outflow of Beijing city air. *J. Geophys. Res.*, **114**, D00G04, doi: 10.1029/2008JD010780.

Guo, L., E. J. Highwood, L. C. Shaffrey, et al., 2013: The effect of regional changes in anthropogenic aerosols on rainfall of the East Asian summer monsoon. *Atmos. Chem. Phy.*, **13**, 1521–1534.

Han, Y. M., J. J. Cao, B. Z. Yan, et al., 2011: Comparison of elemental carbon in lake sediments measured by three different methods and 150-yr pollution history in eastern China. *Environ. Sci. Technol.*, **45**, 5287–5293.

Hansen, J., M. Sato, R. Ruedy, et al., 2007: Climate simulations for 1880–2003 with GISS modelE. *Climate Dyn.*, **29**, 661–696.

He, X., C. C. Li, A. K. H. Lau, et al., 2009: An intensive study of aerosol optical properties in Beijing urban area. *Atmos. Chem. Phy.*, **9**, 8903–8915.

IPCC, 2013: *Summary for Policymakers. Climate change 2013: The Physical Science Basis. Contribution of Working Group I to the Fifth Assessment Report of the Intergovernmental Panel on Climate Change*, Stocker, T. F., D. Qin, G.-K. Plattner, et al., Eds., Cambridge University Press, Cambridge, United Kingdom and New York, NY, USA, 2216 pp.

Jacobson, M. Z., 2004: Climate response of fossil fuel and biofuel soot, accounting for soot's feedback to snow and sea ice albedo and emissivity. *J. Geophys. Res.*, **109**, D21201, doi: 10.1029/2004JD004945.

Jacobson, M. Z., 2005: Correction to control of fossil-fuel particulate black carbon and organic matter, possibly the most effective method of slowing global warming. *J. Geophys. Res.*, **110**, D14105, doi: 10.1029/2005JD005888.

Janssens, I. A., W. Dieleman, S. Luyssaert, et al., 2010: Reduction of forest soil respiration in response to nitrogen deposition. *Nature Geoscience*, **3**, 315–322.

Jiang, H., H. Liao, H. O. T. Pye, et al., 2013: Projected effect of 2000–2050 changes in climate and emissions on aerosol levels in China and associated transboundary transport. *Atmos. Chem. Phy.*, **13**, 7937–7960.

Jiang Yiquan, Liu Xiaohong, Yang Xiuqun, et al., 2013: A numerical study of the effect of different aerosol types on East Asian summer clouds and precipitation. *Atmos. Environ.*, **70**, 51–63.

Kaufman, Y. J., B. N. Holben, D. Tanré, et al., 2000: Will aerosol measurements from Terra and Aqua polar orbiting satellites represent the daily aerosol abundance and properties? *Geophys. Res. Lett.*, **27**, 3861–3864.

Kim, D.-H., B.-J. Sohn, T. Nakajima, et al., 2004: Aerosol optical properties over East Asia determined from ground-based sky radiation measurements. *J. Geophys. Res.*, **109**, D02209, doi: 10.1029/2003JD003387.

Koch, D., M. Schulz, S. Kinne, et al., 2009: Evaluation of black carbon estimations in global aerosol models. *Atmos. Chem. Phy.*, **9**, 9001–9026.

Kopacz, M., D. L. Mauzerall, J. Wang, et al., 2011: Origin and radiative forcing of black carbon transported to the Himalayas and Tibetan Plateau. *Atmos. Chem. Phy.*, **11**, 2837–2852, doi: 10.5194/acp-11-2837-2011.

Lamarque, J.-F., J. T. Kiehl, G. P. Brasseur, et al., 2005: Assessing future nitrogen deposition and carbon cycle feedback using a multimodel approach: Analysis of nitrogen deposition. *J. Geophys. Res.*, **110**, D19303, doi: 10.1029/2005JD005825.

Lee, K. H., Z. Q. Li, M. S. Wong, et al., 2007: Aerosol single scattering albedo estimated across China from a combination of ground and satellite measurements. *J. Geophys. Res.*, **112**, D22S15, doi: 10.1029/2007JD009077.

Li, C., L. T. Marufu, R. R. Dickerson, et al., 2007: In situ measurements of trace gases and aerosol optical properties at a rural site in northern China during East Asian study of tropospheric aerosols: An international regional experiment 2005. *J. Geophys. Res.*, **112**, D22S04, doi: 10.1029/2006JD007592.

Li Xingsheng, He Zhuanshi, Fang Xiumei, et al., 1999: Distribution of surface ozone concentration in the clean areas of China and its possible impact on crop yields. *Adv. Atmos. Sci.*, **16**, 154–158.

Li, Z. Q., H. Chen, M. Cribb, et al., 2007: Preface to special section on East Asian studies of tropospheric aerosols: An international regional experiment (EAST-AIRE). *J. Geophys. Res.*, **112**, D22S04, doi: 10.1029/2006JD007592.

Liao, H., and J. H. Seinfeld, 2005: Global impacts of gas-phase chemistry-aerosol interactions on direct radiative forcing by anthropogenic aerosols and ozone. *J. Geophys. Res.*, **110**, D18208, doi: 10.1029/2005JD005907.

Liao, H., W.-T. Chen, and J. H. Seinfeld, 2006: Role of climate change in global predictions of future tropospheric ozone and aerosols. *J. Geophys. Res.*, **111**, D12304, doi: 10.1029/2005jd006852.

Liao Hong and Chang Wenyuan, 2014: Integrated assessment of air quality and climate change for policy-making: Highlights of IPCC AR5 and research challenges. *National Science Review*, **1**, 176–179, doi: 10.1093/nsr/nwu005.

Lin, W., X. Xu, X. Zhang, et al., 2008: Contributions of pullutants from North China Plain to surface ozone at the Shangdianzi GAW Station. *Atmos. Chem. Phy.*, **8**, 5889–5898.

Liu, X., K. Chang, C. E. Sioris, et al., 2006: First directly retrieved global distribution of tropospheric column ozone from GOME: Comparison with the GEOS-CHEM model. *J. Geophys. Res.*, **111**, D02308, doi: 10.1029/2005JD006564.

Liu Jianjun, Zheng Youfei, Li Zhanqing, et al., 2008: Ground-based remote sensing of aerosol optical properties in one city in Northwest China. *Atmos. Res.*, **89**, 194–205.

Lou Sijia, Liao Hong, and Zhu Bin, 2014: Impacts of aerosols on surface-layer ozone concentrations in China through heterogeneous reactions and changes in photolysis rates. *Atmos. Environ.*, **85**, 123–138.

Lu, Z., Q. Zhang, and D. G. Streets, 2011: Sulfur dioxide and primary carbonaceous aerosol emissions in China and India, 1996–2010. *Atmos. Chem. Phy.*, **11**, 9839–9864.

Lyapustin, A., A. Smirnov, B. Holben, et al., 2011: Reduction of aerosol absorption in Beijing since 2007 from MODIS and AERONET. *Geophys. Res. Lett.*, **38**, L10803, doi: 10.1029/2011GL047306.

Ma Jinghui, Zheng Youfei, and Zhang Hua, 2007: The optical depth global distribution of black carbon aerosol and its possible reason analysis. *Scientia Meteor. Sinica*, **27**, 549–556. (in Chinese)

Ma, N., C. S. Zhao, A. Nowak, et al., 2011: Aerosol optical properties in the North China Plain during HaChi campaign: An in-situ optical closure study. *Atmos. Chem. Phy.*, **11**, 5959–5973.

Meng, Z. Y., X. B. Xu, P. Yan, et al., 2009: Characteristics of trace gaseous pollutants at a regional background station in northern China. *Atmos. Chem. Phy.*, **9**, 927–936.

Menon, S., J. Hansen, L. Nazarenko, et al., 2002: Climate effects of black carbon aerosols in China and India. *Science*, **297**, 2250–2253.

Menon, S., D. Koch, G. Beig, et al., 2010: Black carbon aerosols and the third polar ice cap. *Atmos. Chem. Phy.*, **10**, 4559–4571, doi: 10.5194/acp-10-4559-2010.

Ming, J., H. Cachier, C. Xiao, et al., 2008: Black carbon record based on a shallow Himalayan ice core and its climatic implications. *Atmos. Chem. Phy.*, **8**, 1343–1352.

Müller, D., M. Tesche, H. Eichler, et al., 2006: Strong particle light absorption over the Pearl River Delta (South China) and Beijing (North China) determined from combined Raman lidar and Sun photometer observations. *Geophys. Res. Lett.*, **33**, L20811, doi: 10.1029/2006GL027196.

Prather, M. J., C. D. Holmes, and J. Hsu, 2012: Reactive greenhouse gas scenarios: Systematic exploration of uncertainties and the role of atmospheric chemistry. *Geophys. Res. Lett.*, **39**, L09803, doi: 10.1029/2012GL051440.

Qin, Y., and S. D. Xie, 2011: Estimation of county-level black carbon emissions and its spatial distribution in China in 2000. *Atmos. Environ.*, **45**, 6995–7004.

Qin, Y., and S. D. Xie, 2012: Spatial and temporal variation of anthropogenic black carbon emissions in China for the period 1980–2009. *Atmos. Chem. Phy.*, **12**, 4825–4841.

Qiu Jinhuan, Yang Liquan, and Zhang Xiaoye, 2004: Characteristics of the imaginary part and single-scattering albedo of urban aerosols in northern China. *Tellus B*, **56**, 276–284.

Qiu Jinhuan and Yang Jingmei, 2008: Absorption properties of urban/suburban aerosols in China. *Adv. Atmos. Sci.*, **25**, 1–10.

Qu Wenjun, Zhang Xiaoye, Wang Yaqiang, et al., 2006: The physical and chemical characterization of carbonaceous aerosol at the atmospheric background site in Diqing, Yunnan. *China Environ. Sci.*, **26**, 266–270. (in Chinese)

Qu Wenjun, Wang Jun, Gao Shanhong, et al., 2013: Effect of the strengthened western Pacific subtropical high on summer visibility decrease over eastern China since 1973. *J. Geophys. Res.*, **118**, 7142–7156, doi: 10.1002/jgrd.50535.

Ramanathan, V., P. J. Crutzen, J. T. Kiehl, et al., 2001: Aerosols, climate, and the hydrological cycle. *Science*, **294**, 2119–2124.

Shindell, D., J. C. I. Kuylenstierna, E. Vignati, et al., 2012: Simultaneously mitigating near-term climate change and improving human health and food security. *Science*, **335**, 183–189.

Stevenson, D. S., F. J. Dentener, M. G. Schultz, et al., 2006: Multimodel ensemble simulations of present-day and near-future tropospheric ozone. *J. Geophys. Res.*, **111**, D08301, doi: 10.1029/2005JD006338.

Takami, A., W. Wang, D. G. Tang, et al., 2006: Measurements of gas and aerosol for two weeks in northern China during the winter-spring period of 2000, 2001, and 2002. *Atmos. Res.*, **82**, 688–697.

Tang, G., X. Li, Y. Wang, et al., 2009: Surface ozone trend details and interpretations in Beijing, 2001–2006. *Atmos. Chem. Phy.*, **9**, 8813–8823.

Tu Jun, Xia Zongguo, Wang Hesheng, et al., 2007: Temporal variations in surface ozone and its precursors and meteorological effects at an urban site in China. *Atmos. Res.*, **85**, 310–337.

UNEP, 2011: *Integrated Assessment of Black Carbon and Tropospheric Ozone: Summary for Decision Makers.* Nairobi, UNON, Publishing Services Section, 36 pp.

Wang Rong, Tao Shu, Wang Wentao, et al., 2012: Black carbon emissions in China from 1949 to 2050. *Environ. Sci. Technol.*, **46**, 7595–7603.

Wang, T., H. L. A. Wong, J. Tang, et al., 2006: On the origin of surface ozone and reactive nitrogen observed at a remote mountain site in the northeastern Qinghai-Tibetan Plateau, western China. *J. Geophys. Res.*, **111**, D08303, doi: 10.1029/2005JD006527.

Wang Tijian, Xie Min, Gao Lijie, et al., 2004: Development and preliminary application of a coupled regional climate-chemistry model system. *J. Nanjing Univ. (Nat. Sci.)*, **40**, 711–727. (in Chinese)

Wang Weiguo, Wu Jian, Liu Hongnian, et al., 2005: Researches on the influence of pollution emission on tropospheric ozone variation and radiation over China and its adjacent area. *Chinese J. Atmos. Sci.*, **29**, 734–746. (in Chinese)

Wang Xin, Xu Baiqing, and Ming Jing, 2014: An overview of the studies on black carbon and mineral dust deposition in snow and ice cores in East Asia. *J. Meteor. Res.*, **28**, 354–370, doi: 10.1007/s13351-014-4005-7.

Wang, Y., Y. Zhang, J. Hao, et al., 2011: Seasonal and spatial variability of surface ozone over China: Contributions from background and domestic pollution. *Atmos. Chem. Phy.*, **11**, 3511–3525.

Wang Yuxuan, Shen Lulu, Wu Shiliang, et al., 2013: Sensitivity of surface ozone over China to 2000–2050 global changes of climate and emissions. *Atmos. Environ.*, **75**, 374–382, doi: 10.1016/j.atmosenv.2013.04.045.

Wang Yuesi, Xin Jinyuan, Pan Yuepeng, et al., 2014: The Campaign on atmospheric Aerosol REsearch network of China: CARE-China. *Bull. Amer. Meteor. Soc.*, doi: 10.1175/BAMS-D-14-00039.1.

Wang Zhili, Guo Pinwen, and Zhang Hua, 2009: A numerical study of direct radiative forcing due to black carbon and its effects on the summer precipitation in China. *Climatic Environ. Res.*, **14**, 161–171. (in Chinese)

Wang Zhili, Zhang Hua, and Shen Xueshun, 2011: Radiative forcing and climate response due to black carbon in snow and ice. *Adv. Atmos. Sci.*, **28**, 1336–1344, doi: 10.1007/s00376-011-0117-5.

Wendisch, M., O. Hellmuth, A. Ansmann, et al., 2008: Radiative and dynamic effects of absorbing aerosol particles over the Pearl River Delta, China. *Atmos. Environ.*, **42**, 6405–6416.

Wild, O., and H. Akimoto, 2001: Intercontinental transport of ozone and its precursors in a three-dimensional global CTM. *J. Geophys. Res.*, **106**, 27729–27744.

Wu, J., C. Fu, Y. Xu, et al., 2008: Simulation of direct effects of black carbon aerosol on temperature and hydrological cycle in Asia by a Regional Climate Model. *Meteor. Atmos. Phys.*, **100**, 179–193.

Xia Xiang'ao, Chen Hongbin, Wang Pucai, et al., 2005: Aerosol properties and their spatial and temporal variations over North China in spring 2001. *Tellus B*, **57**, 28–39.

Xia, X. A., H. B. Chen, P. C. Wang, et al., 2006: Variation of column-integrated aerosol properties in a Chinese urban region. *J. Geophys. Res.*, **111**, D05204, doi: 10.1029/2005JD006203.

Xu, B. Q., J. J. Cao, J. Hansen, et al., 2009: Black soot and the survival of Tibetan glaciers. *Proc. Nat. Acad. Sci. USA*, **106**, 22114–22118.

Xu, J., M. H. Bergin, X. Yu, et al., 2002: Measurement of aerosol chemical, physical and radiative properties in the Yangtze Delta region of China. *Atmos. Environ.*, **36**, 161–173.

Xu Jin, M. H. Bergin, R. Greenwald, et al., 2004: Aerosol chemical, physical, and radiative characteristics near a desert source region of Northwest China during ACE-Asia. *J. Geophys. Res.*, **109**, D19S03, doi: 10.1029/2003JD004239.

Xu, J., J. Z. Ma, X. L. Zhang, et al., 2011: Measurements of ozone and its precursors in Beijing during summertime: Impact of urban plumes on ozone pollution in downwind rural areas. *Atmos. Chem. Phy.*, **11**, 12241–12252.

Xu, X., W. Lin, T. Wang, et al., 2008: Long-term trend of surface ozone at a regional background station in eastern China during 1991–2006: Enhanced variability. *Atmos. Chem. Phy.*, **8**, 2595–2607.

Xu Xiaoguang, Wang Jun, D. K. Henze, et al., 2013: Constraints on aerosol sources using GEOS-Chem adjoint and MODIS radiances, and evaluation with multisensor (OMI, MISR) data. *J. Geophys. Res.*, **118**, 6396–6413, doi: 10.1002/jgrd.50515.

Yan Peng, Li Xingsheng, Luo Chao, et al., 1997: Observational analysis of surface O_3, NO_x, and SO_2 in China. *J. Appl. Meteor. Sci.*, **8**, 53–61. (in Chinese)

Yan Peng, Wang Mulin, Cheng Hongbing, et al., 2003: Distributions and variations of surface ozone in Changshu, Yangtze Delta region. *Acta Metallurgica Sinica*, **17**, 205–217.

Yan, P., J. Tang, J. Huang, et al., 2008: The measurement of aerosol optical properties at a rural site in northern China. *Atmos. Chem. Phy.*, **8**, 2229–2242.

Yu Xingna, Zhu Bin, and Zhang Meigen, 2009: Seasonal variability of aerosol optical properties over Beijing. *Atmos. Environ.*, **43**, 4095–4101.

Zhang Hua, Ma Jinghui, and Zheng Youfei, 2008: The study of global radiative forcing due to black carbon aerosol. *Chinese J. Atmos. Sci.*, **32**, 1147–1158. (in Chinese)

Zhang Hua, Wang Zhili, Guo Pinwen, et al., 2009: A modeling study of the effects of direct radiative forcing due to carbonaceous aerosol on the climate in East Asia. *Adv. Atmos. Sci.*, **26**, 57–66.

Zhang Hua, Wang Zhili, Wang Zaizhi, et al., 2012: Simulation of direct radiative forcing of aerosols and their effects on East Asian climate using an interactive AGCM-aerosol coupled system. *Climate Dyn.*, **38**, 1675–1693, doi: 10.1007/s00382-011-1131-0.

Zhang Hua, Xie Bing, Zhao Shuyun, et al., 2014: $PM_{2.5}$ and tropospheric O_3 in China and an analysis of the impact of pollutant emission control. *Adv. Climate Change Res.*, **5**, 136–141.

Zhang Li, Liao Hong, and Li Jianping, 2010a: Impacts of Asian summer monsoon on seasonal and interannual variations of aerosols over eastern China. *J. Geophys. Res.*, **115**, D00K05, doi: 10.1029/2009JD012299.

Zhang, L., H. Liao, and J. Li, 2010b: Impact of the Southeast Asian summer monsoon strength on the outflow of aerosols from South Asia. *Annales Geophysicae*, **28**, 277–287.

Zhang, Q., D. G. Streets, G. R. Carmichael, et al., 2009: Asian emissions in 2006 for the NASA INTEX-B mission. *Atmos. Chem. Phy.*, **9**, 5131–5153.

Zhang, X. Y., Y. Q. Wang, D. Wang, et al., 2005: Characterization and sources of regional-scale transported carbonaceous and dust aerosols from different pathways in coastal and sandy land areas of China. *J. Geophys. Res.*, **110**, D15301, doi: 10.1029/2004JD005457.

Zhang, X. Y., Y. Q. Wang, X. C. Zhang, et al., 2008b: Carbonaceous aerosol composition over various regions of China during 2006. *J. Geophys. Res.*, **113**, D14111, doi: 10.1029/2007JD009525.

Zhuang Bingliang, Wang Tijian, and Li Shu, 2009: The first indirect radiative forcing of black carbon aerosol and its effect on regional climate of China. *Plateau Meteor.*, **28**, 1095–1104. (in Chinese)

Zhuang, B. L., L. Liu, F. H. Shen, et al., 2010a: Semidirect radiative forcing of internal mixed black carbon cloud droplet and its regional climatic effect over China. *J. Geophys. Res.*, **115**, D00K19, doi: 10.1029/2009JD013165.

Zhuang Bingliang, Jiang Fei, Wang Tijian, et al., 2010b: Investigation on the direct radiative effect of fossil fuel black-carbon aerosol over China. *Theor. Appl. Climatol.*, **104**, 301–312.

Zhuang Bingliang, Liu Qian, Wang Tijian, et al., 2013: Investigation on semi-direct and indirect climate effects of fossil fuel black carbon aerosol over China. *Theor. Appl. Climatol.*, **114**, 651–672.

Zhuang, B. L., T. J. Wang, S. Li, et al., 2014: Optical properties and radiative forcing of urban aerosols in Nanjing, China. *Atmos. Environ.*, **83**, 43–52.